

Heavy Ions and Generalized Nuclear Recoils in Xenon with NEST v2.0

Jacob Cutter, University of California, Davis
On Behalf of the NEST Collaboration

v1.3: August 20, 2019

When discussing nuclear recoil models in NEST, we are typically discussing the limiting case where the recoiling nucleus is the same species as the surrounding medium (e.g. xenon yields light and charge in response to a recoiling xenon nucleus). However, we have also developed a model for arbitrary nuclei recoiling through xenon, as from nuclear decay of intruding radioactive isotopes. Here we will examine the case where $Z_1 \neq Z_2$ and $A_1 \neq A_2$ (indices 1 and 2 will hereafter refer to the recoiling nucleus and the species of the medium, respectively).

According to Lindhard theory [3], there is a characteristic energy E_c (E_{1c} and E_{2c} for the two species) at which the nuclear and electronic stopping powers are similar in the medium, i.e. $S_n \sim S_e$. This quantity naturally provides different regimes for approximation; for $E < E_c$ the contribution from nuclear stopping dominates (very little energy goes into electronic motion), and for $E > E_c$ the electronic stopping dominates.

Since most cases of interest to us are within the low-energy regime, we will use the former approximation. Lindhard defines the characteristic energies E_{1c} , E_{2c} , and E_c as

$$E_{1c} \approx \frac{A_1^3 \left(Z_1^{2/3} + Z_2^{2/3} \right)^2}{(A_1 + A_2)^2 Z_1^{1/3}} \cdot (500 \text{ eV})$$

$$E_{2c} \approx \frac{(A_1 + A_2)^2 Z_2}{A_1} \cdot (125 \text{ eV})$$

$$E_c = \gamma E_{2c}, \quad \gamma = \frac{4A_1 A_2}{(A_1 + A_2)^2}$$

and provides an approximate numerical solution for the sum of energy given to electronic excitation (for the case $E < E_{1c}$, E_{2c}):

$$\eta = \frac{2}{3} \left(\frac{1}{\sqrt{E_{1c}}} + \frac{1}{2} \sqrt{\frac{\gamma}{E_c}} \right) E^{3/2} \quad (1)$$

Then, the Lindhard factor, or the fraction of energy lost to electronic excitation, is

$$L(E, A_1, Z_1, A_2, Z_2) = \frac{\eta}{E} = \frac{2}{3} \left(\frac{1}{\sqrt{E_{1c}}} + \frac{1}{2\sqrt{E_{2c}}} \right) \sqrt{E} \quad (2)$$

This Lindhard factor is then used to model the yield of total quantum in NEST. However, we do find that the energy dependence of Eq. 2 leads to insufficient quenching (i.e. too many predicted quanta) in some cases. It is difficult to estimate where a nucleus becomes too heavy or energetic to use the above Lindhard factor, however we modify the Lindhard factor with an additional constraint in the high-energy limit.

The datasets of Doke, Tanaka, and Hitachi et al. for Lindhard quenching of high energy ions (n , α , ^{12}C , Ne, Si, Ar, Fe, ^{206}Pb , and ^{252}Cf) [1][2][4] are used to model the atomic mass dependence of the Lindhard factor in the high energy limit. This function then serves as an upper bound on the Lindhard factor used by NEST. The atomic mass dependence of this L_{max} is given by

$$L_{\text{max}}(A) = \frac{a}{1 + (A^2/b)^c} \quad (a = 0.96446, b = 19227, c = 0.99199) \quad (3)$$

This parametrized fit to data is shown in Fig. 1.

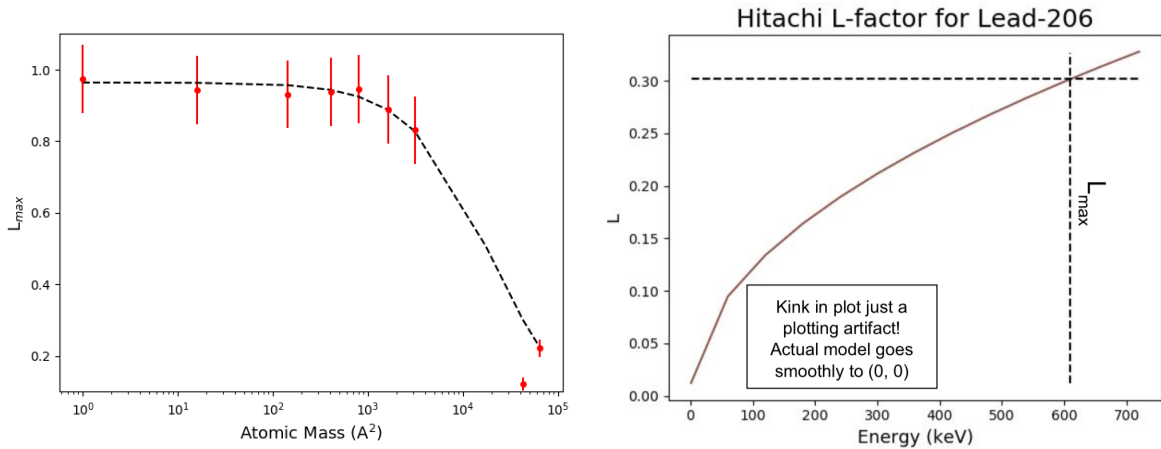


Figure 1: (Left) The atomic mass dependence of L_{max} (dotted line) used as an upper bound on the calculated Lindhard factor, along with heavy ion data (red dots). (Right) The energy-dependent Lindhard factor for a ^{206}Pb nucleus.

Data for α particles is more readily available from xenon experiments across a broad range of energies, and thus they are treated as a special case. For these nuclei, the empirical Lindhard factor takes the form of a power law in energy:

$$L_{\alpha} = a E^b \quad (a = 0.56136, b = 0.056972) \quad (4)$$

We would intuitively expect the number of protons in a nucleus to play a role in liberating electrons from Xe nuclei. This motivates the use of an atomic number-dependent power law for the exciton-ion ratio, i.e. the initial partitioning of quanta:

$$\frac{N_{ex}}{N_i} = \alpha + a Z^b, \quad \alpha = \frac{c}{(1 + (\rho/10)^2)^d} \quad (5)$$

$$(a = 0.00178, b = 1.587, c = 0.64, d = 449.61)$$

where α is a density-dependent parameter which becomes non-negligible for noble elements in the gas phase and ρ is the mass density of the medium.

From the Lindhard factor L and the exciton-ion ratio, it is possible to calculate both the total number of quanta N_q and the number of initial ions created N_i :

$$N_q = \frac{L \cdot E}{W}$$

$$N_i = \frac{N_q}{1 + N_{ex}/N_i} \quad (6)$$

A modified Thomas-Imel box (TIB) model is used to determine the recombination probability for both the α and heavy ion models, which then allows calculation of the resulting numbers of photons and electrons. The TIB parameter is dependent on density, atomic mass, and electric field. The dependence on field is intuitive, since the electric field pulls electrons from the interaction site and prevents recombination.

The origin of the atomic mass dependence is related to the ionization density in the recoil track; the species of the nucleus determines the stopping power and the resulting track structure, and the sparseness of the track further determines local screening (shielding) of the electric field by the ion cloud. Furthermore, there should be an additional dependence on the density of the medium, since this further influences the track structure.

The density dependence is an empirical power law of the density:

$$D_\rho = \left(\frac{\rho}{a}\right)^b \quad (a = 0.2679, b = -2.3245) \quad (7)$$

To extrapolate from α particles to larger nuclei, an empirically derived exponential mass dependence term is also used. This is found by fitting charge yields from α , ^{206}Pb , and Xe-Xe nuclear recoil data:

$$D_A = a e^{b(A/4-1)} + c \quad (8)$$

($a = 0.02966094$, $b = 0.17687876$, $c = 1.0 - 0.02966094$)

The field dependence of recombination is a power law of the electric field given by

$$D_F = \begin{cases} \left[1 + \left(\frac{F}{a}\right)^b\right]^c & \text{(Liquid Phase)} \\ \sqrt{F} & \text{(Gas Phase)} \end{cases} \quad (9)$$

$$(a = 95., b = 8.7, c = 0.0592)$$

The resulting TIB parameter then takes the overall form

$$\xi = \frac{a D_A}{D_F (1 + D_\rho)} \quad (a = 0.00625) \quad (10)$$

This TIB parameter is used to calculate the recombination probability (which is of course restricted to be $\in [0, 1]$):

$$R = 1 - \frac{4 \ln(1 + N_i \xi/4)}{N_i \xi} \quad (11)$$

The resulting number of photons N_{ph} and number of electrons N_e are then

$$N_{ph} = \frac{N_q \cdot N_{ex}/N_i}{1 + N_{ex}/N_i} + R N_i$$

$$N_e = N_q - N_{ph} \quad (12)$$

To validate the heavy ion model, we start by cross-checking the high-energy NEST predictions with the original Doke and Tanaka datasets for various nuclei (see Fig. 2). While one dataset is systematically lower than the other, the NEST curve is shown to roughly split the difference. Within the quoted errors, the NEST model matches data well; this is due to the implementation of a maximum Lindhard factor constraint at high energies (as shown, these datasets include relativistic ions at 422 MeV and above).

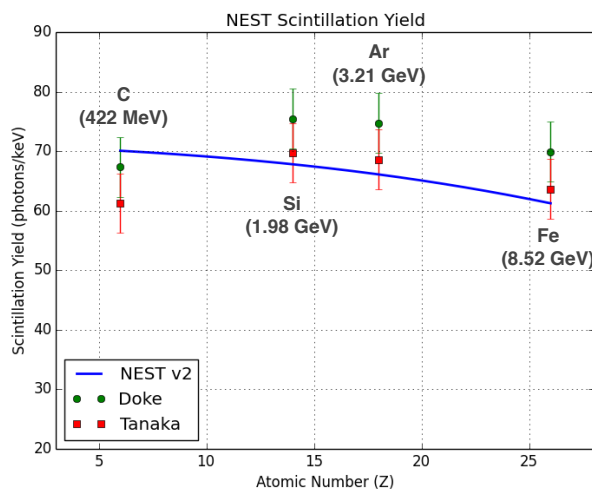


Figure 2: The NEST v2 model (blue) compared with the original Doke (green) and Tanaka (red) data used to constrain L_{\max} .

We would like to demonstrate these models at all energies, and compare the response of various nuclei. This is non-trivial, as there are dependencies of the model on atomic number, atomic mass, energy, and electric field. Furthermore, real physical isotopes come in different stable configurations, i.e. with different neutron mass fractions.

To maintain the utility of these models, we calculate the light and charge yields (normalized by energy) for naturally occurring isotopes, taking into account natural abundances by using the average atomic mass. In Fig. 3, we can see that while differences in the atomic mass distribution for each isotope results in crossing points of the light yield curves, there is an overall reduction in the light yield as atomic mass increases (at the same energy).

Additionally, there are notable “kinks” in the light yield curve for each isotope, generally at higher energy for larger nuclei, where the light yield becomes very flat. This is due to a moving saturation point, an energy at which the Lindhard reaches its constrained maximum value, resulting in a simple linear energy dependence. The charge yield is much smoother, since it is only a small fraction of the total quantum yield, and is less sensitive to sudden changes in the Lindhard factor dependence. Also note that the well-known light and charge anti-correlation is maintained here, hidden by the axis scales.

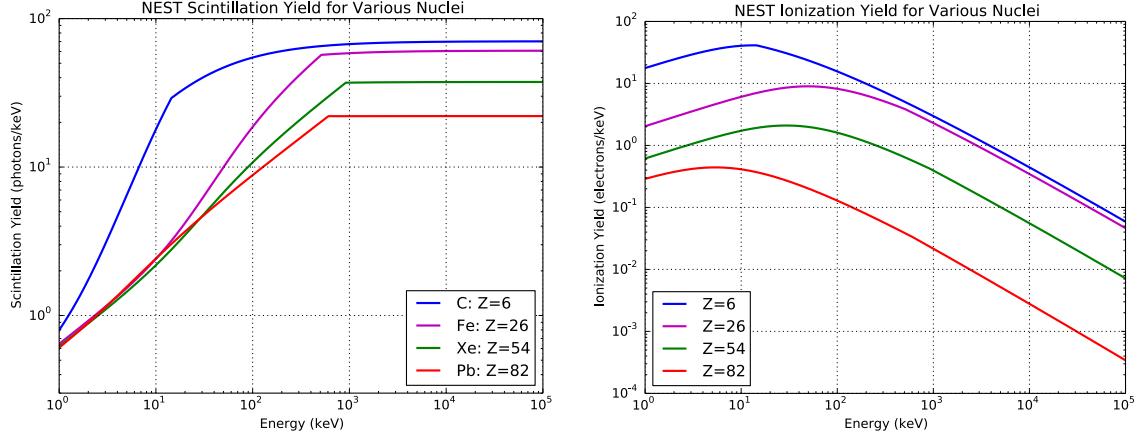


Figure 3: (Left) Normalized light yield (photons per keV) for natural isotopes of C, Fe, Xe, and Pb. (Right) Normalized charge yields (electrons per keV) for the same isotopes.

We can additionally take a given species, where the number of protons stays constant, and study the dependence of the light and charge yields on the atomic mass for different isotopes. Shown in Fig. 4 are the yields for various fields, as a function of their natural decay energies.

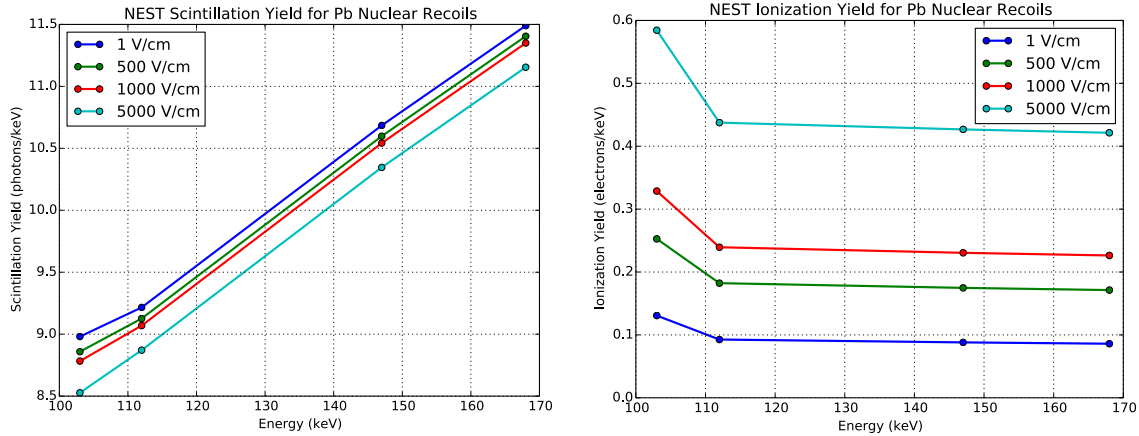


Figure 4: (Left) Normalized light yield (photons per keV) for real Pb isotopes resulting from nuclear decays, for various electric fields. (Right) Normalized charge yields (electrons per keV) for the same nuclei.

Even here, it is non-trivial to compare isotopes, since there is not a simple relationship between isotopes and the kinetic energies of the nuclei resulting from natural radioactive decays. While the above curves are monotonic due to the energy dependence of the model, the dependence on atomic mass is complicated. For example, the ordering of the isotopes in this plot is: ^{206}Pb , ^{214}Pb , ^{210}Pb , ^{208}Pb .

It is also worth noting that the field dependence is relatively weak for large nuclei, since the electron fraction is already so small due to the nuclear recoil track structure, field screening effects, and strong recombination. However, the plots do show a monotonic decrease in

the light yield as a function of field, and an appropriate increase in the charge yield due to stronger electron drift; this of course makes sense, given the anticorrelation due to light production by recombination.

References

- [1] Tadayoshi Doke, Akira Hitachi, Jun Kikuchi, Kimiaki Masuda, Hiroyuki Okada, and Eido Shibamura. Absolute scintillation yields in liquid argon and xenon for various particles. *Japanese Journal of Applied Physics, Part 1: Regular Papers and Short Notes and Review Papers*, 2002.
- [2] Akira Hitachi. Properties of liquid xenon scintillation for dark matter searches. *Astroparticle Physics*, 2005.
- [3] J Lindhard, V Nielsen, and M Scharff. Integral equations governing radiation effects. *Mat. Fys. Medd. Dan. Vid. Selsk.*, 1963.
- [4] M. Tanaka, T. Doke, A. Hitachi, T. Kato, J. Kikuchi, K. Masuda, T. Murakami, F. Nishikido, H. Okada, K. Ozaki, E. Shibamura, and E. Yoshihira. LET dependence of scintillation yields in liquid xenon. *Nuclear Instruments and Methods in Physics Research, Section A: Accelerators, Spectrometers, Detectors and Associated Equipment*, 2001.